Chapter 5

A Newton Linearized Two-Level Alternating Direction Implicit Scheme for Two-Dimensional Nonlinear Time Fractional Reaction–Diffusion Equation on a Bounded Domain

5.1 Introduction

In this chapter, we apply the Newton linearized alternating direction implicit scheme based on the $L2-1_\sigma$ interpolation approximation [110] on graded meshes for solving two-dimensional time fractional reaction–diffusion equation with Dirichlet boundary condition on a bounded domain,

$$\begin{cases} {}_0^C D_t^{\alpha} u(x,y,t) = \Delta u(x,y,t) + f(u(x,y,t)) + F(x,y,t), & (x,y,t) \in \Omega \times (0,T], \\ u(x,y,0) = \phi_1(x,y), & (x,y) \in \Omega, \\ u(x,y,t) = \phi_2(x,y,t), & (x,y) \in \partial\Omega, t \in (0,T], \end{cases} \tag{5.1}$$

where, $\Omega = (0,L) \times (0,L) \subset \mathbb{R}^2$ is a bounded and convex polygon in $\mathbb{R}^2$, $\alpha \in (0,1)$, F is the sufficiently smooth known function and $f(u)$ is a nonlinear function known as reaction term such that it satisfies the Lipschitz condition

$$|f(u_1) - f(u_2)| \leq L|u_1 - u_2|,$$

where L is a positive Lipschitz constant.

This study presents an effective numerical method for solving time fractional nonlinear reaction–diffusion equation. In the process of developing the scheme, the time fractional derivative is approximated using the $L2-1_\sigma$ scheme on the graded meshes, and spatial discretization is done using central difference approximation. The nonlinear reaction term is approximated by using the second-order Newton linearization method. Further, in order to reduce the computational cost for solving the two-dimensional problem, an alternating direction implicit algorithm is applied whose main advantage is that it reduces the multi-dimensional problem to a set of independent one-dimensional problems. Various types of fractional differential equations are being solved by the researchers using alternating direction implicit methods such as [111, 112, 113, 114]. finally the unique solvability, stability, and convergence of the scheme are discussed.

In summary, the main contributions of this work are:

- A fully discrete alternating direction implicit scheme is developed for solving (5.1) using $L2-1_{\sigma}$ formula and standard central difference approximation.
- Due to the presence of the initial layer at $t=0$, in the solution of nonlinear time fractional PDEs, smoothly graded meshes are considered for the discretization of the temporal domain.
- The stability and convergence of the scheme are studied rigorously. The finite difference scheme is proved to have $(1+\alpha)$ order convergence for smooth solution and α order convergence for nonsmooth solution in temporal direction and second order convergence in spatial direction.

The outline of this chapter is as follows: in Section 5.2, we propose a linearized alternating direction implicit scheme for solving (5.1) and discuss the regularity conditions of the solution. Unique solvability, stability, and error estimates of the fully discrete scheme are discussed in Section 5.3. In Section 5.4, numerical experimentation is done to validate the theoretical findings. Finally, in Section 5.5, some concluding remarks are given.

5.2 Fully Discrete Alternating Direction Implicit Scheme

By choosing the positive integer M as temporal partition parameter, we discretize the time domain $[0,T]$ as $0=t_0<t_1<t_2<\cdots<t_M=T$, with step size $\tau_j=t_j-t_{j-1}$, $j=1,2,\cdots M$. For $0\leq\sigma<1$ define $t_{k-\sigma}=t_k-\sigma\tau_k$. For positive integers M_1 and M_2 as spatial partition parameters, we set the spatial mesh as $x_n=nh_x$, $n=0,1,\cdots,M_1$ and $y_m=mh_y$, $m=0,1,2,\cdots,M_2$. The space-time mesh is $(x_n, y_m, t_{k-\sigma})$, $n = 0, 1, \cdots, M_1$, $m = 0, 1, 2, \cdots, M_2$, $k = 1, \cdots, M$. Let $\bar{\Omega}_h$ be the set of discrete grids such that $\bar{\Omega}_h = \{(x_n, y_m) : 0 \le n \le M_1, 0 \le m \le M_2\}$, $\Omega_h = \bar{\Omega}_h \cap \Omega$ and $\partial\Omega_h = \bar{\Omega}_h \cap \partial\Omega$. Define local step size ratio $\rho_k = \frac{\tau_k}{\tau_{k+1}}$ and $\tau = \max_{1\le j\le N} |\tau_j|$. For any sequence of functions $\{\phi^k\}$, define $\nabla_\tau \phi^k = \phi^k - \phi^{k-1}$ and $\phi^{k,\sigma} = (1-\sigma)\phi^k + \sigma\phi^{k-1}$.

To discretize the Caputo time fractional derivative, we use the well-known $L2-1_\sigma$ formula [110]. So we have,

$$
\begin{aligned}
{}_0^C D_t^\alpha u^{k-\sigma} &= \int_0^{t_{k-\sigma}} \omega_{1-\alpha}(t_{k-\sigma} - s) u'(s) ds \\
&= \sum_{j=1}^{k-1} \int_{t_{j-1}}^{t_j} \omega_{1-\alpha}(t_{k-\sigma} - s) u'(s) ds + \int_{t_{k-1}}^{t_{k-\sigma}} \omega_{1-\alpha}(t_{k-\sigma} - s) u'(s) ds.
\end{aligned}
$$

Let $P_{1,j}u$ be the linear interpolate of u at the nodes t_{j-1}, t_j (2.1) and $P_{2,j}u$ be the quadratic interpolate of u at the nodes t_{j-1} and t_j and t_{j+1} (2.10). So we have

$$
\begin{aligned}
{}_0^C D_t^\alpha u^{k-\sigma} =& \sum_{j=1}^{k-1} \int_{t_{j-1}}^{t_j} \omega_{1-\alpha}(t_{k-\sigma} - s)(P_{2,j}u)'(s) ds + \int_{t_{k-1}}^{t_{k-\sigma}} \omega_{1-\alpha}(t_{k-\sigma} - s)(P_{1,j})'(s) ds \\
=& \sum_{j=1}^{k-1} \int_{t_{j-1}}^{t_j} \omega_{1-\alpha}(t_{k-\sigma} - s) \left[\frac{\nabla_\tau u^j}{\tau_j} + \frac{2(s - t_{j-1/2})}{\tau_j(\tau_j + \tau_{j+1})} (\rho_j \nabla_\tau u^{j+1} - \nabla_\tau u^j) \right] ds \\
&+ \int_{t_{k-1}}^{t_{k-\sigma}} \omega_{1-\alpha}(t_{k-\sigma} - s) \frac{\nabla_\tau u^k}{\tau_k} ds, \\
=& a_0^{(k)} \nabla_\tau u^k + \sum_{j=1}^{k-1} \left(a_{k-j}^{(k)} \nabla_\tau u^j + \rho_j b_{k-j}^{(k)} \nabla_\tau u^{j+1} - b_{k-j}^{(k)} \nabla_\tau u^j \right), \qquad (5.2) \\
=& - A_{k-1}^{(k)} u^0 + \sum_{j=1}^{k-1} \left(A_{k-j-1}^{(k)} - A_{k-j}^{(k)} \right) u^j \\
&+ A_0^{(k)} u^k + \mathcal{O}(\tau^{3-\alpha}), \;\; k = 1, 2, \cdots, M, \qquad (5.3)
\end{aligned}
$$

where $a_0^k = \frac{1}{\tau_k} \int_{t_{k-1}}^{t_{k-\sigma}} \omega_{1-\alpha}(t_{k-\sigma} - s) ds$,

$a_{k-j}^k = \frac{1}{\tau_j} \int_{t_{j-1}}^{t_j} \omega_{1-\alpha}(t_{k-\sigma} - s) ds$,

$b_{k-j}^{k} = \frac{2}{\tau_j(\tau_j+\tau_{j+1})}\int_{t_{j-1}}^{t_j}(s-t_{j-1/2})\omega_{1-\alpha}(t_{k-\sigma}-s)ds,$

and

$$A_{k-j}^{(k)} = \begin{cases} a_{k-1}^{(k)} - b_{k-1}^{(k)}, & j=1, \\ a_{k-j}^{(k)} + \rho_{j-1}b_{k-j+1}^{(k)} - b_{k-j}^{(n)}, & 2 \le j \le k-1, \\ a_0^{(k)} + \rho_{k-1}b_1^{(k)}, & j=k. \end{cases}$$

The diffusion terms are approximated by standard second order discretization,

$$u_{xx}(x_n, y_m, t_{k-\sigma}) \approx \delta_x^2 u_{n,m}^{k-\sigma} + \mathcal{O}(h_x^2) \text{ and } u_{yy}(x_n, y_m, t_{k-\sigma}) \approx \delta_y^2 u_{n,m}^{k-\sigma} + \mathcal{O}(h_y^2).$$

So we have,

$$-A_{k-1}^{(k)}u_{n,m}^0 + \sum_{j=1}^{k-1}(A_{k-j-1}^{(k)} - A_{k-j}^{(k)})u_{n,m}^j + A_0^{(k)}u_{n,m}^k = \delta_x^2 u_{n,m}^{k-\sigma} + \delta_y^2 u_{n,m}^{k-\sigma} + f(u_{n,m}^{k-\sigma}) + F(x_n, y_m, t_{k-\sigma}). \quad (5.4)$$

Lemma 5.2.1. For $\varsigma(t) \in C^3[0, t_k],\ k = 1, 2, \cdots, M$ and for any $\alpha \in (0, 1)$ we have,

$$\varsigma(t_{k-\sigma}) = \sigma\varsigma(t_{k-1}) + (1-\sigma)\varsigma(t_k). \quad (5.5)$$

Proof. Using Taylor's expansion formula, we obtain

$$\begin{aligned}\varsigma(t_{k-\sigma}) =& \varsigma(t_k - \sigma\tau_k) \\ =& \varsigma(t_k) - \sigma\tau_k\varsigma'(t_k) + \mathcal{O}(\tau^2), \\ =& (1-\sigma)\varsigma(t_k) + \sigma(\varsigma(t_k) - \tau_k\varsigma'(t_k) + \mathcal{O}(\tau^2)) + (1-\sigma)\mathcal{O}(\tau^2), \\ =& (1-\sigma)\varsigma(t_k) + \sigma\varsigma(t_k - \tau_k) + \mathcal{O}(\tau^2), \\ =& (1-\sigma)\varsigma(t_k) + \sigma\varsigma(t_{k-1}) + \mathcal{O}(\tau^2).\end{aligned}$$

□

The nonlinear term $f(u_{n,m}^{k-\sigma})$ is approximated as,

$$f(u_{n,m}^{k-\sigma}) = f(u_{n,m}^{k-1}) + (1-\sigma)f'(u_{n,m}^{k-1})(u_{n,m}^{k} - u_{n,m}^{k-1}). \tag{5.6}$$

From (5.4), (5.5) and (5.6), we have

$$\begin{aligned} A_0^{(k)}u_{n,m}^k - (1-\sigma)\delta_x^2 u_{n,m}^{k+1} - (1-\sigma)\delta_y^2 u_{n,m}^{k+1} - (1-\sigma)f'(u_{n,m}^{k-1})u_{n,m}^k \\ = A_{k-1}^{(k)}u_{n,m}^0 + \sigma(\delta_x^2 u_{n,m}^{k-1} + \delta_y^2 u_{n,m}^{k-1}) + f(u_{n,m}^{k-1}) - (1-\sigma)f'(u_{n,m}^{k-1})u_{n,m}^{k-1} \\ + \sum_{j=1}^{k-1}\left(A_{k-j-1}^{(k)} - A_{k-j}^{(k)}\right)u_{n,m}^j + F(x_n, y_m, t_{k-\sigma}). \end{aligned} \tag{5.7}$$

Let $A_0^k - (1-\sigma)f'(u_{n,m}^k) = \varrho$ and dividing both sides of (5.7) by ϱ we get,

$$\begin{aligned} u_{n,m}^k - \frac{(1-\sigma)}{\varrho}(\delta_x^2 + \delta_y^2)u_{n,m}^k = \frac{1}{\varrho}\Bigg(A_{k-1}^{(k)}u_{n,m}^0 + \sigma(\delta_x^2 u_{n,m}^{k-1} + \delta_y^2 u_{n,m}^{k-1}) + f(u_{n,m}^{k-1}) \\ - (1-\sigma)f'(u_{n,m}^{k-1})u_{n,m}^{k-1} + \sum_{j=1}^{k-1}\left(A_{k-j-1}^{(k)} - A_{k-j}^{(k)}\right)u_{n,m}^j + F(x_n, y_m, t_{k-\sigma})\Bigg). \end{aligned}$$

To construct the alternating direction implicit scheme, we add the perturbation term $\frac{(1-\sigma)^2}{\varrho^2}\delta_x^2\delta_y^2(u_{n,m}^k - u_{n,m}^{k-1})$ so we get,

$$\begin{aligned} \left(1 - \frac{(1-\sigma)}{\varrho}\delta_x^2\right)\left(1 - \frac{(1-\sigma)}{\varrho}\delta_y^2\right)u_{n,m}^k = \frac{(1-\sigma)^2}{\varrho^2}\delta_x^2\delta_y^2 u_{n,m}^{k-1} + \frac{1}{\varrho}\Bigg(A_{k-1}^{(k)}u_{n,m}^0 \\ + \sigma(\delta_x^2 u_{n,m}^{k-1} + \delta_y^2 u_{n,m}^{k-1}) + f(u_{n,m}^{k-1}) - (1-\sigma)f'(u_{n,m}^{k-1})u_{n,m}^{k-1} \\ + \sum_{j=1}^{k-1}\left(A_{k-j-1}^{(k)} - A_{k-j}^{(k)}\right)u_{n,m}^j + F(x_n, y_m, t_{k-\sigma})\Bigg). \end{aligned} \tag{5.8}$$

Omitting the small error terms, we obtain the following numerical scheme,

$$\left(1-\frac{(1-\sigma)}{\varrho}\delta_x^2\right)\left(1-\frac{(1-\sigma)}{\varrho}\delta_y^2\right)U_{n,m}^k=\frac{(1-\sigma)^2}{\varrho^2}\delta_x^2\delta_y^2u_{n,m}^{k-1}+\varphi_{n,m}^{k-1}, \tag{5.9}$$

where

$$\begin{aligned}\varphi_{n,m}^{k-1}=&\frac{1}{\varrho}\Bigg(A_{k-1}^{(k)}u_{n,m}^0+\sigma(\delta_x^2u_{n,m}^{k-1}+\delta_y^2u_{n,m}^{k-1})+f(u_{n,m}^{k-1})-(1-\sigma)f'(u_{n,m}^{k-1})u_{n,m}^{k-1}\\&+\sum_{j=1}^{k-1}\left(A_{k-j-1}^{(k)}-A_{k-j}^{(k)}\right)u_{n,m}^j+g(x_n,y_m,t_{k-\sigma})\Bigg).\end{aligned} \tag{5.10}$$

By introducing the intermediate variable $U_{n,m}^*=\left(1-\frac{(1-\sigma)}{\varrho}\delta_y^2\right)U_{n,m}^k$, we obtain the following two-level linearized alternating direction implicit scheme,

$$\left(1-\frac{(1-\sigma)}{\varrho}\delta_x^2\right)U_{n,m}^*=\varphi_{n,m}^{k-1}+\frac{(1-\sigma)^2}{\varrho^2}\delta_x^2\delta_y^2u_{n,m}^{k-1}, \tag{5.11}$$

$$\left(1-\frac{(1-\sigma)}{\varrho}\delta_y^2\right)U_{n,m}^k=U_{n,m}^*. \tag{5.12}$$

The typical solutions of nonlinear time fractional PDEs have an initial layer extensively described by [115, 95],

$$\left|\frac{\partial^l u}{\partial x^l}(x,t)\right|\le C,\ l=0,\ 1,\ 2,\ 3,\ 4, \tag{5.13}$$

$$\left|\frac{\partial^m u}{\partial t^m}(x,t)\right|\le C(1+t^{\alpha-m}),\ \alpha\in(0,1)\cup(1,2),\ m=1,\ 2,\ 3, \tag{5.14}$$

where C is a constant.

Remark 5.2.1. As discussed in [93, 95], if $\phi_1\in H_0^1(\Omega)\cap H^2(\Omega)$, for every t and $f(u)$ is Lipschitz continuous then (5.1) has a unique solution u such that,

$$u\in C^\alpha([0,T];L^2(\Omega))\cap C([0,T];H_0^1(\Omega)\cap H^2(\Omega)),$$

Remark 5.2.2. To tackle the initial singularities, we assume some restrictions on the temporal step sizes. Let $C_r > 0$ be a constant independent of k and $r \geq 1$ is fixed such that,

$$\tau_k \leq C_r \tau \min\{1, t_k^{1-1/r}\},\ 1 \leq k \leq M, t_k \leq C_r t_{k-1} \text{ and}$$
$$\tau_k/\tau_{k-1} \leq C_r\ t_k/t_{k-1},\ 2 \leq k \leq N. \tag{5.15}$$

Due to the presence of initial layer in the solution of nonlinear time fractional PDEs assumption (5.15) is necessary. Graded meshes are one of the examples of the meshes that satisfy the condition given in (5.15). On any given interval $[0, T^*]$, graded meshes are defined as,

$$t_k = T^* \left(\frac{k}{M_0}\right)^r,\ k = 0,\ 1, \cdots, M_0,$$

where M_0 is a positive integer and $r \geq 1$ is the grading parameter adapted to the strength of the singularity.

5.3 Stability and Convergence of the Alternating Direction Implicit Scheme

The coefficient matrices in both the system of equations (5.11) and (5.12) are strictly diagonally dominant which ensures the uniqueness and existence of solution of the finite difference scheme.

5.3.1 Stability Analysis

Now we will discuss the stability of the finite difference scheme using von Neumann stability analysis. We introduce the perturbation term $\tau_{n,m}^k$ to the finite difference scheme (5.9) and examine how the perturbation term $\tau_{n,m}^k = U_{n,m}^k - \hat{U}_{n,m}^k$, propagates with time, where $\hat{U}_{n,m}^k$ is the solution of the perturbed system. So we have,

$$\begin{aligned}\left(1-\frac{(1-\sigma)}{\varrho}\delta_x^2\right)\left(1-\frac{(1-\sigma)}{\varrho}\delta_y^2\right)(U_{n,m}^k-\hat{U}_{n,m}^k) &= \frac{(1-\sigma)^2}{\varrho^2}\delta_x^2\delta_y^2(U_{n,m}^{k-1}-\hat{U}_{n,m}^{k-1})\\ &+\frac{1}{\varrho}\Bigg(A_{k-1}^{(k)}(U_{n,m}^0-\hat{U}_{n,m}^0)+\sigma\left(\delta_x^2(U_{n,m}^{k-1}-\hat{U}_{n,m}^{k-1})+\delta_y^2(U_{n,m}^{k-1}-\hat{U}_{n,m}^{k-1})\right)\\ &+f(U_{n,m}^{k-1})-f(\hat{U}_{n,m}^{k-1})-(1-\sigma)\left(f'(U_{n,m}^{k-1})U_{n,m}^{k-1}-f'(\hat{U}_{n,m}^{k-1})\hat{U}_{n,m}^{k-1}\right)\\ &+\sum_{j=1}^{k-1}\left(A_{k-j-1}^{(k)}-A_{k-j}^{(k)}\right)\left(U_{n,m}^{j}-U_{n,m}^{j-1}\right)\Bigg).\end{aligned}$$

Using the Lipschitz property of the function f, we have

$$\begin{aligned}\left(1-\frac{(1-\sigma)}{\varrho}\delta_x^2\right)\left(1-\frac{(1-\sigma)}{\varrho}\delta_y^2\right)\tau_{n,m}^k &= \frac{(1-\sigma)^2}{\varrho^2}\delta_x^2\delta_y^2\tau_{n,m}^{k-1}+\frac{1}{\varrho}\Bigg(A_{k-1}^{(k)}\tau_{n,m}^0\\ &+\sigma(\delta_x^2\tau_{n,m}^{k-1}+\delta_y^2\tau_{n,m}^{k-1})+L\tau_{n,m}^{k-1}-C(1-\sigma)\tau_{n,m}^{k-1}\\ &+\sum_{j=1}^{k-1}(A_{k-j-1}^{(k)}-A_{k-j}^{(k)})\tau_{n,m}^{j-1}\Bigg). \qquad (5.16)\end{aligned}$$

To apply the von Neumann stability analysis, let $\tau_{n,m}^k = \xi^k e^{i\omega_1 nh_x + i\omega_2 mh_y}$, where ω_1 and ω_2 are wave numbers. Note that,

$$\begin{aligned}\delta_x^2\tau_{n,m}^k &= -\frac{4}{h_x^2}\sin^2\left(\frac{\omega_1 h_x}{2}\right)\xi^k e^{i\omega_1 nh_x+i\omega_2 mh_y} = \lambda_1\xi^k e^{i\omega_1 nh_x+i\omega_2 mh_y},\\ \delta_y^2\tau_{n,m}^k &= -\frac{4}{h_y^2}\sin^2\left(\frac{\omega_2 h_y}{2}\right)\xi^k e^{i\omega_1 nh_x+i\omega_2 mh_y} = \lambda_2\xi^k e^{i\omega_1 nh_x+i\omega_2 mh_y}.\end{aligned}$$

We have from (5.16),

$$\left(1+\frac{(1-\sigma)}{\varrho}\lambda_1\right)\left(1+\frac{(1-\sigma)}{\varrho}\lambda_2\right)\xi^k = \frac{(1-\sigma)^2}{\varrho^2}\lambda_1\lambda_2\xi^{k-1} + \frac{1}{\varrho}\Bigg(A^{(k)}_{k-1}\xi^0 + \sigma(\lambda_1+\lambda_2)\xi^{k-1} + L\xi^{k-1} - C(1-\sigma)\xi^{k-1} + \sum_{j=1}^{k-1}(A^{(k)}_{k-j-1} - A^{k}_{k-j})\xi^{j-1}\Bigg),$$

$$\xi^k = \frac{1}{\left(1+\frac{(1-\sigma)}{\varrho}\lambda_1\right)\left(1+\frac{(1-\sigma)}{\varrho}\lambda_2\right)}\Bigg(\frac{(1-\sigma)^2}{\varrho^2}\lambda_1\lambda_2\xi^{k-1} + \frac{1}{\varrho}\big(A^{(k)}_{k-1}\xi^0 + \sigma(\lambda_1+\lambda_2)\xi^{k-1} + L\xi^{k-1} - C(1-\sigma)\xi^{k-1} + \sum_{j=1}^{k-1}(A^{(k)}_{k-j-1} - A^{(k)}_{k-j})\xi^{j-1}\big)\Bigg).$$

Now, by using the idea of mathematical induction we show that $|\xi^k| \leq |\xi^0|$ for all k.

For $k = 1$ we have,

$$|\xi^1| \leq \frac{1}{\left(1+\frac{(1-\sigma)}{\varrho}\lambda_1\right)\left(1+\frac{(1-\sigma)}{\varrho}\lambda_2\right)}\Bigg(\frac{(1-\sigma)^2}{\varrho^2}\lambda_1\lambda_2 + \frac{1}{\varrho}\big(A^{(k)}_{k-1} + \sigma(\lambda_1+\lambda_2) + L - C(1-\sigma)\big)\Bigg)|\xi^0|,$$

observe that, $1-\sigma,\ \sigma \geq 0$ and $1-\sigma \leq \sigma,\ C_{k,0} \geq 0$. So we have,

$$|\xi^1| \leq \frac{1}{\left(1+\frac{(1-\sigma)}{\varrho}\lambda_1\right)\left(1+\frac{(1-\sigma)}{\varrho}\lambda_2\right)}\left(\frac{(1-\sigma)^2}{\varrho^2}\lambda_1\lambda_2 + 1 + \frac{(1-\sigma)}{\varrho}(\lambda_1+\lambda_2)\right)|\xi^0|,$$

$$|\xi^1| \leq |\xi^0|.$$

Let $|\xi^k| \leq |\xi^0|$ for $k = 1, 2, \cdots, s-1$. For $k = s$,

$$|\xi^s| = \frac{1}{\left(1+\frac{(1-\sigma)}{\varrho}\lambda_1\right)\left(1+\frac{(1-\sigma)}{\varrho}\lambda_2\right)}\Bigg(\frac{(1-\sigma)^2}{\varrho^2}\lambda_1\lambda_2\xi^{s-1} + \frac{1}{\varrho}\big(A^{(s)}_{s-1}\xi^0 + \sigma(\lambda_1+\lambda_2)\xi^{s-1}$$

$$
\begin{aligned}
&+ L\xi^{s-1} - C(1-\sigma)\xi^{s-1} + \sum_{j=1}^{s-1}(A^{(s)}_{s-j-1} - A^{(s)}_{s-j})\xi^j\Big)\,,\\
\leq & \frac{1}{\left(1+\frac{(1-\sigma)}{\varrho}\lambda_1\right)\left(1+\frac{(1-\sigma)}{\varrho}\lambda_2\right)}\left[\frac{(1-\sigma)^2}{\varrho^2}\lambda_1\lambda_2 + \frac{(1-\sigma)}{\varrho}(\lambda_1+\lambda_2) + \frac{L}{\varrho}\right.\\
&\left. - \frac{C(1-\sigma)}{\varrho} + \frac{A^{(s)}_0}{\varrho}\right]|\xi^0|,\\
\leq & \frac{1}{\left(1+\frac{(1-\sigma)}{\varrho}\lambda_1\right)\left(1+\frac{(1-\sigma)}{\varrho}\lambda_2\right)}\left[\frac{(1-\sigma)^2}{\varrho^2}\lambda_1\lambda_2 + \frac{(1-\sigma)}{\varrho}(\lambda_1+\lambda_2) + 1\right]|\xi^0|,\\
\leq & |\xi^0|.
\end{aligned}
$$

5.3.2 Error Estimate

The discrete coefficients $A^{(k)}_{k-j}$ satisfy the following properties proved in [116, 117]

P1: Discrete coefficients are monotone, i.e., $0 < A^{(k)}_{k-1} < A^{(k)}_{k}$, $1 \leq k \leq M$.

P2: There exist a positive constant π_A such that,

$$A^{(k)}_{k-j} \geq \frac{1}{\pi_A \tau_j}\int_{t_{j-1}}^{t_j} \omega_{1-\alpha}(t_k - s)ds, 1 \leq j \leq k \leq M.$$

P3: There exist a constant $\rho > 0$ such that the local step size ratio $\rho_n \leq \rho$, $1 \leq n \leq M$. With the help of these properties, we define the complimentary discrete convolution kernel and get the following lemmas.

Lemma 5.3.1. [115] Let the coefficients

$$P^{(k)}_0 := \frac{1}{A^{(k)}_0}, \quad P^{(k)}_{k-j} := \frac{1}{A^{(j)}_0}\sum_{n=j+1}^{k}(A^{(n)}_{n-j-1} - A^{(n)}_{n-j})P^{(k)}_{k-n},\ 1 \leq j \leq k-1, \quad (5.17)$$

then it holds,

$$\sum_{j=1}^{k} P^{(k)}_{k-j}\omega_{1-\alpha}(t_j) \leq \pi_A,\ 1 \leq k \leq M,$$

and

$$\sum_{j=1}^{k} P_{k-j}^{(k)} \leq t_k^{\alpha} \pi_A \Gamma(2-\alpha). \tag{5.18}$$

Lemma 5.3.2. [115] For any sequence $\{\phi^k\}_{k=0}^{M}$, it holds that,

$$\frac{1}{2}\sum_{j=1}^{k} A_{k-j}^{(k)} \nabla_\tau(\|\phi^j\|^2) \leq \langle \phi^{k,\sigma}, (D_\tau^\alpha \phi)^{k-\sigma} \rangle \rangle, \text{ for } 1 \leq k \leq M. \tag{5.19}$$

Lemma 5.3.3. [115] Suppose that the nonnegative sequences $\{\phi_1^k, \phi_2^k\}_{k=0}^{M}$ satisfy,

$$\sum_{j=1}^{k} A_{k-j}^{(k)} \nabla_\tau(\phi_1^j)^2 \leq \lambda_1(\phi_1^k)^2 + \lambda_2(\phi_1^{k-1})^2 + \phi_1^{k,\sigma}(\phi_2^K + \eta), \; k \geq 1. \tag{5.20}$$

Then it holds that,

$$\phi_1^k \leq 2E_\alpha\left(2\max(1,\rho)\pi_A \lambda t_K^\alpha\right)\left[\phi_1^0 + \max_{1\leq j\leq k}\sum_{n=1}^{j} P_{j-n}^{(j)}\phi_2^n + \pi_A\Gamma(2-\alpha)t_k^\alpha \eta\right], \tag{5.21}$$

where τ_k satisfies $\max_{1\leq k\leq M}\tau_k \leq (2\pi_A\Gamma(2-\alpha)\lambda)^{\frac{-1}{\alpha}}$, $\lambda = \lambda_1 + \lambda_2$.

Lemma 5.3.4. [116] Suppose that $\phi \in C^3(0,T]$ and there exist a constant $C_\phi > 0$ such that,

$$|\phi'''(t)| \leq C_\phi(1 + t^{m-3}), \text{ for } 0 \leq t \leq T.$$

Then it holds that

$$\sum_{j=1}^{k} P_{k-j}^{(k)}|\gamma_1^j| \leq C_\phi\left(\frac{\tau_1^m}{m} + \max_{2\leq n\leq k} t_n^{m-(3-\alpha)/r}\tau^{3-\alpha}\right),$$

where $\gamma_1^j = \frac{1}{\Gamma(1-\alpha)}\int_0^{t_{j-\sigma}} \frac{\phi'(s)}{(t-s)^\alpha}ds - (D_\tau^\alpha \phi(t))^{j-\sigma}$.

To study the detailed error estimate, we need to introduce the following discrete system,

$$ {}_0^C D_\tau^\alpha U_{n,m}^{k-\sigma} = \Delta U_{n,m}^{k,\sigma} - f(U_{n,m}^{k-1}) - (1-\sigma) f'(U_{n,m}^{k-1})(U_{n,m}^{k} - U_{n,m}^{k-1}). \tag{5.22} $$

Let $\epsilon_{n,m}^k = U_{n,m}^k - u_{n,m}^k$, $(x_n, y_m) \in \bar{\Omega}_h$ and $1 \le k \le M$. So we have

$$ {}_0^C D_\tau^\alpha \epsilon_{n,m}^{k-\sigma} - \Delta \epsilon_{n,m}^{k,\sigma} - r_{n,m}^{k,\sigma} = (E_t)_{n,m}^k + (E_s)_{n,m}^k, \tag{5.23} $$

where $(E_t)_{n,m}^k$ and $(E_s)_{n,m}^k$ represent the truncation errors in time and space directions, respectively. From the regularity assumption (5.13), the second order spatial discretization gives, $\|(E_s)_{n,m}^k\| \le Ch^2$. The term $r_{n,m}^{k,\sigma}$ from Eq. (5.23) is evaluated as,

$$ \begin{aligned} r_{n,m}^{k,\sigma} =& f(U_{n,m}^{k-1}) + (1-\sigma) f'(U_{n,m}^{k-1})(U_{n,m}^{k} - U_{n,m}^{k-1}) - f(u_{n,m}^{k-1}) \\ & - (1-\sigma) f'(u_{n,m}^{k-1})(u_{n,m}^{k} - u_{n,m}^{k-1}), \\ =& f(U_{n,m}^{k-1}) - f(u_{n,m}^{k-1}) + (1-\sigma) f'(U_{n,m}^{k-1}) U_{n,m}^k - (1-\sigma) f'(u_{n,m}^{k-1}) U_{n,m}^k \\ & + (1-\sigma) f'(u_{n,m}^{k-1}) U_{n,m}^k - (1-\sigma) f'(u_{n,m}^{k-1}) u_{n,m}^k + (1-\sigma) f'(u_{n,m}^{k-1}) u_{n,m}^{k-1} \\ & - (1-\sigma) f'(U_{n,m}^{k-1}) u_{n,m}^{k-1} + (1-\sigma) f'(U_{n,m}^{k-1}) u_{n,m}^{k-1} \\ & - (1-\sigma) f'(u_{n,m}^{k-1}) u_{n,m}^{k-1}. \end{aligned} \tag{5.24} $$

For $f \in C^2(\mathbb{R})$, there exist a constant $C > 0$ such that,

$$ \|f'(u^{k-1})\| \le C, \tag{5.25} $$

$$ \|f(U^{n-1}) - f(u^{n-1})\| \le C\|\epsilon^{k-1}\|, \tag{5.26} $$

$$ \|f'(U^{n-1}) - f'(u^{n-1})\| \le C\|\epsilon^{k-1}\|. \tag{5.27} $$

From (5.24), (5.25), (5.26) and (5.27), we have,

$$\begin{aligned}\|r^{k,\sigma}_{n,m}\| \leq & C\left[\|\epsilon^{k-1}\| + (1-\sigma)\|U^{k}_{n,m}\|\|\epsilon^{k-1}_{n,m}\| + (1-\sigma)\|\epsilon^{k}_{n,m}\|\|u^{k}_{n,m} + (1-\sigma)\|\epsilon^{k}\|\right. \\ & \left. + (1-\sigma)\|u^{k-1}_{n,m}\|\epsilon^{k-1}_{n,m} + (1-\sigma)\|\epsilon^{k-1}_{n,m}\|\right], \\ \leq & \left[C + (1-\sigma)CC_1 + (1-\sigma)CC_1 + (1-\sigma)C\right]\|\epsilon^{k-1}_{n,m}\| + (1-\sigma)C\|\epsilon^{k}_{n,m}\|, \\ = & C'\left(\|\epsilon^{k-1}_{n,m}\| + \|\epsilon^{k}_{n,m}\|\right). \end{aligned} \tag{5.28}$$

Using Theorem (3.1) of [118]. Taking inner product with $\epsilon^{k,\sigma}_{n,m}$ on (5.23), we have,

$$\begin{aligned}\langle {}^{C}_{0}D^{\alpha}_{\tau}\epsilon^{k-\sigma}_{n,m}, \epsilon^{k,\sigma}_{n,m}\rangle - \langle \Delta\epsilon^{k,\sigma}_{n,m}, \epsilon^{k,\sigma}_{n,m}\rangle = & \langle r^{k,\sigma}_{n,m}, \epsilon^{k,\sigma}_{n,m}\rangle = \langle (E_t)^{k}_{n,m}, \epsilon^{k,\sigma}_{n,m}\rangle \\ & + \langle (E_s)^{k}_{n,m}, \epsilon^{k,\sigma}_{n,m}\rangle.\end{aligned}$$

The positive semidefinite property gives $\langle -\Delta\epsilon^{k,\sigma}_{n,m}, \epsilon^{k,\sigma}_{n,m}\rangle \geq 0$ and from Lemma (5.3.2),

$$\begin{aligned}\frac{1}{2}\sum_{j=1}^{k} A^{k}_{k-j}\nabla_\tau\|\epsilon^{j}_{n,m}\|^2 \leq & \|r^{k,\sigma}_{n,m}\|^2 + \|(E_t)^{k,\sigma}_{n,m}\|\|\epsilon^{k,\sigma}_{n,m}\| + \|(E_s)^{k,\sigma}_{n,m}\|\|\epsilon^{k,\sigma}_{n,m}\|, \\ \leq & C'\left(\|\epsilon^{k-1}_{n,m}\|^2 + \|\epsilon^{k}_{n,m}\|^2\right) + \|\epsilon^{k,\sigma}_{n,m}\|\left(\|(E_t)^{k,\sigma}_{n,m}\| + \|(E_s)^{k,\sigma}_{n,m}\|\right),\end{aligned}$$

using Lemma (5.3.3) and Lemma (5.3.4),

$$\begin{aligned}\|\epsilon^{k}_{n,m}\| \leq & 4E_\alpha\left(2\max(1,\rho)\pi_A\lambda t^{\alpha}_{k}\right)\left[\max_{1\leq j\leq k}\sum_{n=1}^{j} P^{(j)}_{j-n}\|(E_t)^{k,\sigma}_{n,m}\| + \pi_A\Gamma(2-\alpha)t^{\alpha}_{k}Ch^2\right], \\ \leq & 4E_\alpha\left(2\max(1,\rho)\pi_A\lambda t^{\alpha}_{k}\right)\left[C_\phi\left(\frac{\tau_1^m}{m} + \max_{2\leq n\leq k} t_n^{m-(3-\alpha)/r}\tau^{3-\alpha}\right) + t^{\alpha}_{n}h^2\right],\end{aligned}$$

which gives the overall convergence result.

5.4 Numerical Experiments

In the present section, we discuss numerical examples to validate the theoretical findings. For the numerical experimentation of the problem having non smooth solution, we divide the interval $[0, T]$ in two parts, $[0, T^*]$ and $[T^*, T]$ such that $T^* = 2^{-r}$. The first subinterval $[0, T^*]$ is discretized into smoothly graded meshes with $t_k = T^*(\frac{k}{M_0})^r$ for $0 \leq k \leq M_0$ and $M_0 = \frac{rM}{2^r - 1 + r}$. Further, the second subinterval $[T^*, T]$ is discretized with uniform meshes.

Example 5.4.1. Consider the 2-dimensional time fractional Fitzhugh-Nagumo reaction–diffusion equation widely used in modeling transmission of nerve impulses [119],

$$\begin{cases} {}_0^C D_t^\alpha u(x,y,t) - \Delta u(x,y,t) - u(1-u)(u-\theta) = F(x,y,t), & (x,y) \in \Omega,\ 0 < t < 1, \\ u(x,y,0) = \sin(\pi x)\sin(\pi y), & (x,y) \in \Omega, \\ u(x,y,t) = 0, & (x,y) \in \partial\Omega, t \in (0,T], \end{cases}$$

where $\Omega = [0,1]^2$, $0 < \theta < 1$, and F is chosen correspondingly to the exact solution $u(x,y,t) = (1+t^4)\sin(\pi x)\sin(\pi y)$. The given problem has a smooth solution with a nonzero initial condition, so we consider the uniform discretization of the temporal domain by choosing the grading parameter $r = 1$. We calculate the numerical error and convergence order in temporal and spatial directions using the devised finite difference scheme. The obtained results are presented through the Table 5.1, Table 5.2, and Table 5.3. These tables show that the numerical scheme is $(1+\alpha)$th-order accurate in time direction and 2nd-order accurate in space direction. Consider the formulas,

$$\epsilon(h) = \max_{\substack{0 \leq n \leq M_1 \\ 0 \leq m \leq M_2}} \left| U_{n,m}^M(h_x, h_y, \tau) - U_{2n,2m}^M(h_x/2, h_y/2, \tau) \right|, \tag{5.29}$$

$$\epsilon(\tau) = \max_{\substack{0\leq n\leq M_1 \\ 0\leq m\leq M_2}} \left| U^{M}_{n,m}(h_x, h_y, \tau) - U^{2M}_{n,m}(h_x, h_y, \tau/2) \right|, \tag{5.30}$$

where $h = h_x = h_y$. Using (5.29) and (5.30), we graphically validate the convergence order in temporal and spatial directions. We fix $M_1 = M_2 = 400$ and vary $M = 20, 40, 80, 160, 320$, and obtained error using (5.30) is plotted using log-log plot. Similarly, by fixing $M = 320$ and varying $N = 10, 20, 40, 80, 160, 320$, the log-log plot of error using formula (5.29) is shown. Through Fig. 5.1(a), Fig. 5.1(b), and Fig. 5.1(c) we see that the slopes are 1.6, 1.8, and 2, respectively which are in good agreement with theoretical convergence order.

TABLE 5.1: MAE and CO in temporal and spatial directions for α=0.4 for Ex. (5.4.1).

N	$M_1 = M_2 = 500$		$M_1 = M_2$	$N = 5000$	
	MAE	CO		MAE	CO
40	3.52023E-04		2^3	5.87848E-03	
80	1.33837E-04	1.39519	2^4	1.44546E-03	2.02391
160	4.89402E-05	1.45138	2^5	3.49262E-04	2.04914
320	1.75765E-05	1.47736	2^6	7.90387E-05	2.14367

TABLE 5.2: MAE and CO in temporal and spatial directions for α=0.6 for Ex. (5.4.1).

N	$M_1 = M_2 = 500$		$M_1 = M_2$	$N = 5000$	
	MAE	CO		MAE	CO
40	2.17938E-02		2^3	1.14962E-02	
80	7.18899E-03	1.60006	2^4	2.86358E-03	2.00527
160	2.47983E-03	1.53554	2^5	7.16591E-04	1.99860
320	8.76186E-04	1.50093	2^6	1.80541E-04	1.98882

TABLE 5.3: MAE and CO in temporal and spatial directions for α=0.8 for Ex. (5.4.1).

N	$M_1 = M_2 = 500$		$M_1 = M_2$	$N = 5000$	
	MAE	CO		MAE	CO
40	8.16964E-03		2^3	1.11196E-02	
80	2.28879E-03	1.83568	2^4	2.76829E-03	2.00604
160	6.42205E-04	1.83348	2^5	6.90697E-04	2.00287
320	1.82771E-04	1.81299	2^6	1.71937E-04	2.00616

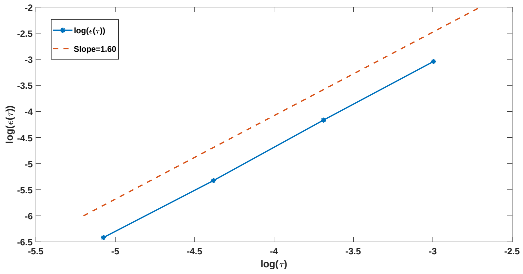

(a) Temporal convergence order for $\alpha = 0.6$

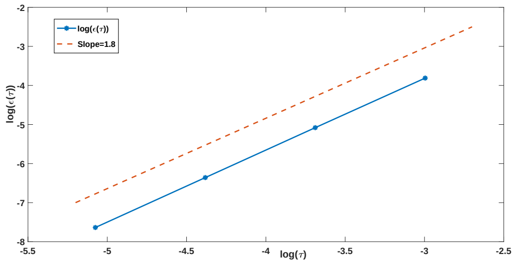

(b) Temporal convergence order for $\alpha = 0.8$

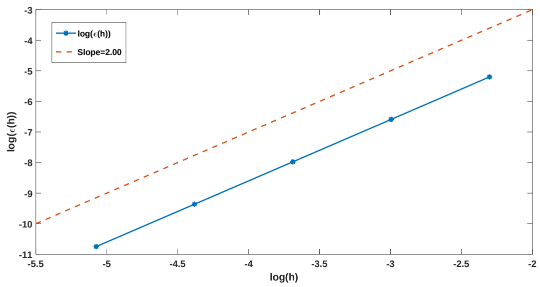

(c) Spatial convergence order for $\alpha = 0.5$

FIGURE 5.1: Convergence order plot in temporal and spatial directions for Ex. 5.4.1.

Example 5.4.2. Consider the following two-dimensional time fractional Fisher's equation being extensively used in ecology, heat and mass transfer [118],

$$ {}_0^C D_t^\alpha u(x,y,t) - \Delta u(x,y,t) - u(1-u^2) = F(x,y,t), \ (x,y) \in [0,2\pi]^2, \ 0 < t < 1, \tag{5.31} $$

the initial and boundary conditions and source term is chosen such that the exact solution is $u(x, y, t) = t^\lambda \sin\big(x/2\big) \sin\big(y/2\big),\ \lambda \in (0, 1)$. The considered example has an initial layer at $t = 0$, so we use smoothly graded meshes to discretize the temporal domain. For different values of $\lambda = \alpha$, convergence order in temporal and spatial directions are calculated with grading parameter $r = 2/\lambda$. The obtained results are presented through Table 5.4, Table 5.5, and Table 5.6. The presented results confirm the αth order temporal accuracy and 2nd order spatial accuracy. Further, the spatial and temporal convergence orders are validated through Fig. 5.2 using formulas (5.29) and (5.30).

TABLE 5.4: MAE and CO in temporal and spatial directions with $r = 2/\lambda$, $\lambda = \alpha = 0.4$ for Ex. 5.4.2.

N	$M_1 = M_2 = 500$		$M_1 = M_2$	$N = 15000$	
	MAE	CO		MAE	CO
10	6.95711E-02		2^3	5.74074E-03	
20	4.97836E-02	4.82817E-01	2^4	1.53352E-03	1.90438
40	3.76240E-02	4.04015E-01	2^5	4.06510E-04	1.91549
80	2.85467E-02	3.98329E-01	2^6	9.70798E-05	2.06604

TABLE 5.5: MAE and CO in temporal and spatial directions with $r = 2/\lambda$, $\lambda = \alpha = 0.6$ for Ex. 5.4.2.

N	$M_1 = M_2 = 500$		$M_1 = M_2$	$N = 15000$	
	MAE	CO		MAE	CO
10	3.56367E-02		2^3	5.74074E-03	
20	2.38411E-02	5.79915E-01	2^4	1.53352E-03	1.90438
40	1.63443E-02	5.44664E-01	2^5	4.06510E-04	1.91549
80	1.09952E-02	5.71904E-01	2^6	9.70798E-05	2.06604

TABLE 5.6: MAE and CO in temporal and spatial directions with $r = 2/\lambda$, $\lambda = \alpha = 0.6$ for Ex. 5.4.2.

N	$M_1 = M_2 = 500$ MAE	$M_1 = M_2 = 500$ CO	$M_1 = M_2$	$N = 15000$ MAE	$N = 15000$ CO
10	1.87663E-02		2^3	5.74075E-03	
20	1.08575E-02	7.89444E-01	2^4	1.53353E-03	1.90438
40	6.21735E-03	8.04331E-01	2^5	4.06510E-04	1.91549
80	3.57763E-03	7.97293E-01	2^6	9.70798E-05	2.06604

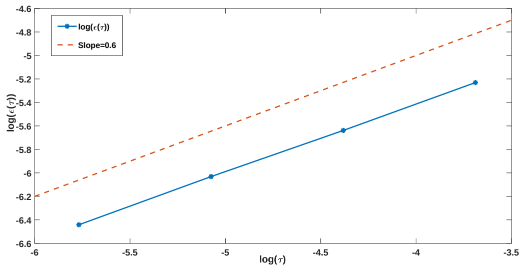

(a) Temporal convergence order for $\alpha = 0.6$

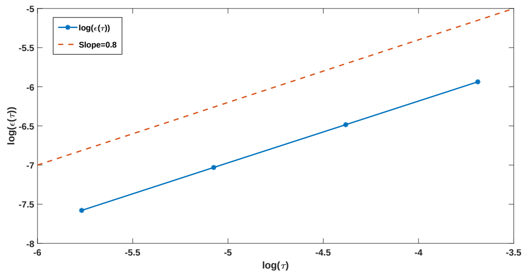

(b) Temporal convergence order for $\alpha = 0.8$

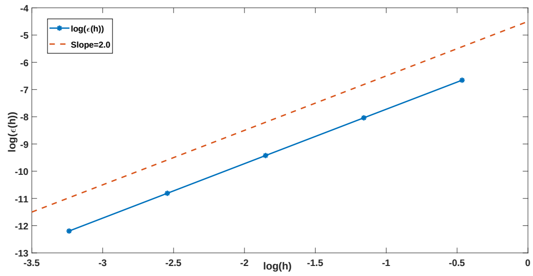

(c) Spatial convergence order for $\alpha = 0.5$

FIGURE 5.2: Convergence order plot in temporal and spatial directions for Ex. 5.4.2.

5.5 Conclusions

In this work, a linearized alternating direction implicit scheme over graded meshes is proposed and analyzed for solving a two-dimensional nonlinear time fractional reaction–diffusion equation having initial layer at $t = 0$. The discussed scheme is proved to be uniquely solvable and stability analysis is discussed using von Neumann stability analysis. The numerical scheme is proved to be convergent with convergence order $(\tau^{1+\alpha}, h^2)$ for smooth solutions and (τ^{α}, h^2) for non smooth solutions. Numerical experimentation is performed on two test examples having smooth and nonsmooth solutions, respectively. The Discussed numerical results validate the theoretical claims.

****